RESEARCH ARTICLE

Underlying microevolutionary processes parallel macroevolutionary patterns in ancient neotropical mountains

Marcos Vinicius Dantas-Queiroz[1] | Tami da Costa Cacossi[2] |
Bárbara Simões Santos Leal[2] | Cleber Juliano Neves Chaves[2] |
Thais N. C. Vasconcelos[3] | Leonardo de Melo Versieux[4] | Clarisse Palma-Silva[1,2]

[1]Programa de Pós-graduação em Biologia Vegetal, Universidade Estadual Paulista (UNESP), Rio Claro, SP, Brazil

[2]Departamento de Biologia Vegetal, Instituto de Biologia, Universidade Estadual de Campinas (UNICAMP), Campinas, SP, Brazil

[3]Department of Biological Sciences, University of Arkansas, Fayetteville, AR, USA

[4]Departamento de Botânica e Zoologia, Centro de Biociências, Universidade Federal do Rio Grande do Norte (UFRN), Natal, RN, Brazil

Correspondence
Marcos Vinicius Dantas-Queiroz, Programa de Pós-graduação em Biologia Vegetal, Universidade Estadual Paulista (UNESP), Rio Claro, SP 13506-900, Brazil.
Email: marvin.danque@gmail.com

Funding information
Funding by CAPES, Grant/Award Number: 88881.128215/2016-01 (MVDQ), PDSE 88881.190071/2018-01 (MVDQ) and PROAP-2015/CAPES/PPGCB-BV); FAPESP, Grant/Award Number: (2018/07596-0 (CPS)); CNPq, Grant/Award Number: produtividade 300819/2016-1 and 305398/2019-9 (CPS); CNPq, Grant/Award Number: produtividade 304778/2013-3 and 303794/2019-4 (LMV); Universal Project, Grant/Award Number: 455510/2014-8 (LMV)

Handling Editor: Sebastien Lavergne

Abstract

Aim: Ancient climatic fluctuations are invoked as the main driving force that generates the astonishing biodiversity in ancient mountains. As a result, endemism and spatial turnover are usually high and few species are widespread amongst entire mountain ranges, precluding the understanding of origins of macroevolutionary patterns. Here, we used a species endemic to, but widespread in, one of the most species-rich ancient mountains in the globe to test how environmental changes acted on and how their macroevolutionary patterns were shaped.

Location: Espinhaço Range, Eastern Brazil.

Taxon: *Vriesea oligantha* species complex (Bromeliaceae).

Methods: We compiled data for plastidial regions and nuclear microsatellites to assess genetic diversity, population structure, migration rates and phylogenetic relationships. Using temperature and precipitation variables, we modelled suitable areas for the present and the past, estimating corridors between isolated populations. We also implemented Bayesian demographic analyses to estimate ancient populations dynamics. Finally, we tested if population structure is driven by isolation by environment or by distance using a Bayesian modelling approach.

Results: Our results showed that the intraspecific divergence events of *V. oligantha* are older than those associated with the latest Pleistocene climatic oscillations, supporting the view that Quaternary climatic fluctuations are key components for understanding its population differentiation processes. Species distribution modelling estimated corridors between populations in the past, as also shown in the demographic analyses, depicting a major spatial reorganization during colder climates. Besides, the high genetic structure estimated results from both models of isolation by distance and by environment.

Main conclusions: *V. oligantha* is a remarkable model to test the effects of climatic oscillations over the biological community, since this species originated in the early-Pleistocene, prevailing over several cycles of climatic fluctuations until today. The estimated demographic dynamics of *V. oligantha* agrees with the species-pump mechanism, suggesting it as the main cause of speciation within the Espinhaço Range. Moreover, the phylogeographic patterns of *V. oligantha* reflect previously recognised

spatial and temporal macroevolutionary patterns in the Espinhaço Range, providing insights into how microevolutionary processes may have given rise to this astonishing mountain biodiversity.

1 | INTRODUCTION

Mountains are remarkable models for evolutionary studies since they host a substantial proportion of the world's biodiversity and harbour high levels of endemism (Antonelli et al., 2018; Perrigo et al., 2020). The drivers of this diversity began to be explored by Alexander von Humboldt, who studied the relationship between mountain vegetation and abiotic factors (Humboldt, 1807), although how this astonishing biodiversity arises is still a debatable subject. Geological processes (i.e. orogeny and erosion) and climate are the most often reported drivers of diversification in mountain ecosystems (Antonelli et al., 2018; Muellner-Riehl et al., 2019; Perrigo et al., 2020). For instance, during mountain uplift, new areas are established, yielding new opportunities for organisms to occupy novel environments and accelerating evolutionary responses (i.e. speciation, extinction, migration, and adaptation) in endemic lineages (Acuña Castillo et al., 2019; Rahbek et al., 2019; Testo et al., 2019). However, while this expectation might be true in mountains of recent orogeny (e.g. the Andes and the Himalayas; Testo et al., 2019; Ye et al., 2019), other lines of evidence are usually adopted to explain the high levels of biodiversity in ancient mountains where uplift has ceased (Rull, 2011; Vasconcelos et al., 2020).

Based on the hypothesis of Quaternary refugia (Haffer, 1969; Vanzolini & Williams, 1970), climatic fluctuations are amongst the main factors that explain the high biodiversity in mountains (Antonelli et al., 2018; Rull, 2011). According to this hypothesis, mountaintops would represent interglacial refugia for species that would have had a much wider distribution at lower elevation during the drier and colder glacial periods. In this scenario, the climate is a strong constraint for species survival, either broadening their potential distribution when the temperatures are lower (i.e. glacial periods) or confining them to areas with milder temperatures, like mountaintops, during interglacial periods, resulting in elevational displacement of species range (Perrigo et al., 2020). This altitudinal displacement may lead to expansion and contraction of suitable habitats and variation in population connectivity (Flantua et al., 2019).

During late Neogene and Pleistocene, pronounced climatic oscillations events took place in the globe, resulting in high vegetation turnover, favoring pulses of expansion and retraction of the montane biological community over time, a phenomenon known as flickering connectivity (Flantua et al., 2019). The concept of flickering connectivity implies continually interconnection and disconnection of adjacent populations associated with shifts of altitudinal limits

(Flantua et al., 2019). This phenomenon might have changed rates of migrants between populations, promoting dispersion pathways to new areas or separating populations into isolated fragments, where isolation may result in allopatric speciation (Flantua & Hooghiemstra, 2018). During the continuous processes of flickering connectivity several populational evolutionary processes, such as genetic drift, local adaptations, secondary contact and hybridization, might ultimately boost the speciation rates of lineages endemic to montane areas, a mechanism called species-pump (Haffer, 1997), biodiversity pump (Rull, 2005), or also known as the isolation-cooling hypothesis (Rull & Vegas-Vilarrúbia, 2020). The species-pump assumes that spatial and environmental isolation are important drivers of speciation, and a presumably consequence is that endemic species are usually restricted to narrow distribution, leading to high spatial turnover (Vasconcelos et al., 2020). This demographic dynamic provides suitable conditions to the emergence of increasing genetic disparity between spatially separated populations due to genetic drift and restricted gene flow as expected in the isolation by distance model (Wright, 1943). On the other hand, local adaptations can also arise in such scenarios, where isolated populations are more prone to exchange migrants between those in more similar environments, regardless of spatial geographic distance (i.e. isolation by environment Sexton et al., 2014; Wang & Bradburd, 2014).

The species-pump mechanism derived from climatic oscillations of the Plio-Pleistocene period was recently evoked to explain the biota formation in the Espinhaço Range, an Eastern South America mountain range (Alcantara et al., 2018; Ribeiro et al., 2014; Vasconcelos et al., 2020). This is because the last major tectonic events that affected these mountains were during Cretaceous period (Dussin & Dussin, 1995; Magalhães Junior et al., 2015) far preceding the diversification of endemic plant lineages in the Espinhaço (Vasconcelos et al., 2020). The Espinhaço Range harbours an astonishing plant diversity, accounting for nearly 15% of the entire Brazilian Flora, with approximately 2000 endemic species, making these mountains home of one of the highest species richness and endemism rates of the world (Silveira et al., 2020). This high degree of endemism associated with different portions of the Espinhaço Range is remarkably congruent between several organisms (Chaves et al., 2015; Echternacht et al., 2011) and has led to the recognition of distinct biogeographical regions in the northern (e.g. the Chapada Diamantina province) and in the mid-southern portions of the range (e.g. the Grão-Mogol, the Diamantina Plateau and the Iron Quadrangle districts; Colli-Silva et al., 2019).

Are past climatic fluctuations common factors that could explain the origin of these congruent biogeographic and diversification patterns in the Espinhaço Range? If the species-pump shaped the macroevolutionary patterns of a given locality, one can expect to observe microevolutionary processes acting at the population level in the early stages of population divergence (Li et al., 2018). Confirming the effects of such processes in already diverged lineages may be challenging, but it might be possible to observe these first steps of speciation in extant populations distributed amongst isolated mountains (Pinheiro et al., 2013). Even though there have been important contributions testing the species-pump hypothesis in several montane areas (e.g. Andes: Sedano & Burns, 2010; Himalayas: Liu et al., 2016; Sierra Nevada: Schoville et al., 2012), the understanding of how underlying microevolutionary processes have promoted the emergence of macroevolutionary patterns of mountains habitats is still to be investigated in ancient mountains with relatively inactive orogeny, such as the Espinhaço Range in Eastern South America.

In this context, we used the widely distributed Espinhaço-endemic bromeliad *Vriesea oligantha* species complex as a model system to investigate how climatic oscillations might have shaped the evolution of endemic lineages in this mountain range. Following the wide distribution and the current suitability in high altitude areas (800–2000 m. a. s. l.) of *V. oligantha*, we hypothesised that its evolutionary history likely follows the history of its habitat, varying in area and connectivity due to ancient climate oscillations. Thus, we predict that (i) isolation by distance together with isolation by environment are the main factors driving diversification, in accordance with the flickering connectivity model, and (ii) population connections might have existed when climate was cooler; while over warmer periods, such connections might have faded. If both hypotheses are corroborated, we would expect that (iii) the genetic structure of populations of *V. oligantha* reflect the macroevolutionary patterns found in other endemic lineages of the Espinhaço Range. To answer these questions, we integrated different approaches, including population genetics, dated phylogenies and ecological niche modelling.

2 | MATERIALS AND METHODS

2.1 | Target taxon, sampling and DNA extraction

The *V. oligantha* complex is composed of *V. oligantha* (Baker) Mez., *V. lancifolia* (Baker) L. B. Sm. and *V. pseudoligantha* Phlicox, a group of plants endemic to the Espinhaço Range. All share similar vegetative and reproductive traits, such as green-greyish leaves, plumose wind-dispersed seeds and nocturnal yellow flowers, which are usually associated with pollination by moths and bats. Such similarities yielded poor taxonomic delimitation over time (Machado et al., 2020; Philcox, 1992), although recent morfo-anatomical traits were in agreement with these taxa (Silva et al., 2020). For the purpose of

this work, we considered all sampled individuals as belonging to the *V. oligantha* species complex.

We sampled 229 individuals from 14 populations of the *V. oligantha* species complex (Table 1) during the years of 2016 and 2017, covering its entire distribution range (Figure 1). Total genomic DNAs were extracted from silica-gel dried leaves following a modified CTAB protocol described by Tel-Zur et al. (1999).

2.2 | Plastidial DNA sequencing and nuclear microsatellite genotyping

Initially, we sequenced six individuals from different populations as a test, using 10 plastidial markers (*petA-psbJ*, *petG-trnC*, *psbA-trnH*, *rpoB-trnC*, *psbM-trnD*, *rpoB-trnC-petN*, *trnK-matK-trnK*, *trnL-trnF*, *ycf1*, *ycf6-trnC*) and one nuclear (*phyC*). From our initial test, we selected two plastidial markers based on their higher polymorphism levels, *ycf1* (Barfuss et al., 2016) and *trnL-trnF* (Barfuss et al., 2005) to be amplified in 95 samples from 14 populations. Amplifications for the *ycf1* and *trnL-trnF* markers were performed in a 30 μl reaction using 3 ng of genomic DNA, 5x GoTaq Green Master Mix (Promega), 0.5 μM of each primer and 1% of DMSO. Polymerase chain reaction (PCR) was conducted using a Veriti 96-well Thermal Cycler (Applied Biosystems) following the protocols described in Barfuss et al. (2005, 2016). PCR products were then purified and sequenced in both forward and reverse directions on Macrogen. Consensus sequences and the alignment matrix were assembled on Geneious R10, using the ClustalW algorithm (Larkin et al., 2007). Indels longer than 1 base pair were removed due to uncertain homology. Both markers were concatenated for subsequent analyses.

For nuclear microsatellites (nrSSR) loci, we genotyped nine polymorphic markers previously transferred from other bromeliads (Cacossi et al., 2019) in 229 individuals from 12 populations. Protocols for genotyping followed those described in Cacossi et al. (2019).

2.3 | Phylogenetic inferences and divergence times

To determine the origin and intraspecific divergence time amongst *V. oligantha* populations, we conducted time calibration analyses in two steps. First, we performed a dating analysis of the Tillandsioideae subfamily, including six individuals of *V. oligantha* from different populations in a matrix with 171 species of Tillandsioideae and seven species from other subfamilies of Bromeliaceae using three plastidial (*matK*, *rpoB-trnC* and *ycf1*) and one nuclear (*phyC*) marker developed by Barfuss et al. (2005, 2016) and downloaded from Genbank. The phylogenetic tree for Tillandsioideae was inferred using the GTR + I + G site model, selected in jModelTest2 (Darriba et al., 2012), assuming a Yule speciation prior. Calibration points were extracted from Givnish et al. (2011) and set as a lognormal distribution prior at the root (19 ± 1.5 Myr) and four other points in the phylogenetic tree

TABLE 1 Population names, geographic locality and tested individual samples for plastidial and nuclear data

Population	Location	Latitude	Longitude	Altitude (m)	Plastidial n	Nuclear n
JAC	Jacobina—BA	−11.1704	−40.5112	713	5	16
MKA	Miguel Calmon—BA	−11.3933	−40.5393	1003	4	−
MCH	Morro do Chapéu—BA	−11.6263	−41.0000	904	6	19
MUC	Mucugê—BA	−12.9915	−41.3440	980	5	19
RCO	Rio de Contas—BA	−13.5244	−41.9567	1577	6	30
ABA	Abaíra—BA	−13.2838	−41.8998	1654	8	19
LIC	Licínio de Almeida—BA	−14.5874	−42.5400	915	5	5
GMO	Grão Mogol—MG	−16.5447	−42.8910	1088	7	20
DIB	Diamantina (Biribiri)—MG	−18.1787	−43.5447	1339	8	20
DIA	Diamantina (Cons. Mata)—MG	−18.3012	−43.8224	1313	6	18
DIM	Diamantina (Milho Verde)—MG	−18.3490	−43.5512	1206	8	−
SGO	São Gonçalo do Rio Preto—MG	−18.1460	−43.3687	906	10	15
CIP	Conceição do Mato Dentro—MG	−19.2467	−43.5116	1270	8	23
OUR	Ouro Branco—MG	−20.5051	−43.6390	1375	9	25

(crown group, 17 ± 1.5 Myr; Tillandsioideae, 16 ± 1.5 Myr; Catopsi deae + Glomeropitcairnieae, 14 ± 1.5 Myr; Vrieseeae, 9 ± 1.5 Myr).

Secondly, using the crown age obtained for the *V. oligantha* clade, we ran a calibration approach to infer the dates of the intraspecific diversification of *V. oligantha*. We used samples from the 95 individuals described above, using seven other Tillandsioideae as outgroups. We used a normal distribution prior for the calibration age at the root, inferred by the previous phylogenetic analysis, the GTR + I + G substitution rate model selected using jModelTest2 and a coalescent constant size random tree under an uncorrelated exponential relaxed-clock model.

Both steps were run in BEAST 1.10.4 and executed in CIPRES Portal (Drummond & Rambaut, 2007; Miller et al., 2010). Each analysis had four independent MCMC runs of 200 million generations sampled every 1000. We used Tracer 1.10.4 (Rambaut et al., 2018) to assess the convergence and effective sample size (ESS > 200) for each run. As a burn-in, we excluded 10% of trees for each step, combining the remaining trees in LogCombiner (available as part of the BEAST package). Maximum clade credibility trees for Tillandsioideae and *V. oligantha* were inferred using TreeAnnotator (Rambaut & Drummond, 2016) and visualised in FigTree 1.4.4 and in the Interactive Tree of Life platform (https://itol.embl.de/).

2.4 | Genetic diversity

For cpDNA, we calculated the nucleotide diversity (π), haplotype diversity (Hd) and polymorphic sites (ss) per population in ARLEQUIN 3.5 (Excoffier & Lischer, 2010). A haplotype matrix was constructed based on ss detected, which were coded as single characters. To explore historical relationships amongst haplotypes, we built a

median-joining-network (Bandelt et al., 1999) on Network 5.0.1.1 (http://www.fluxus-engineering.com).

For nrSSR, putative clones were examined and removed using GenClone 2.0 (Arnaud-Haond & Belkhir, 2006). The number of alleles per locus (A), allelic richness per locus (AR), the observed (H_O) and the expected (H_E) heterozygosity, and the inbreeding coefficient (F_{IS}) were estimated per population using GenAlex 6.5 (Peakall & Smouse, 2012). We evaluated the deviations from the Hardy–Weinberg equilibrium (HWE) per population and per locus using Genepop software v3.5 (Raymond & Rousset, 1995). Linkage disequilibrium between all pairs of loci was tested in FSTAT 2.9.3.2 (Goudet, 1995).

2.5 | Population structure and migration

For the population genetic structure of cpDNA, we employed a clustering with linked loci analysis on BAPS 5.2 (Corander et al., 2008), testing 15 putative clusters. For nrSSR, we used STRUCTURE v.2.3.3 (Pritchard et al., 2000) to assign individuals to genetic clusters (K) under the admixture model assuming independent allele frequencies. The number of K was set from 1 to 13, with 1,000,000 simulations for each K-value and a burn-in rate of 20%. The most probable number of K was examined using Structure Harvester v.6.0 (Earl & von Holdt, 2012), following the instructions of Evanno et al. (2005).

Genetic differentiation was estimated using F-statistics (Weir & Cookham, 1984), based on cpDNA and nrSSR. Pairwise F_{ST} between localities was calculated using ARLEQUIN 3.5. We also conducted a molecular variance analysis (AMOVA) to evaluate the partition genetic variance in hierarchical models grouping by lineages obtained from the phylogenetic cpDNA tree by running 10,000
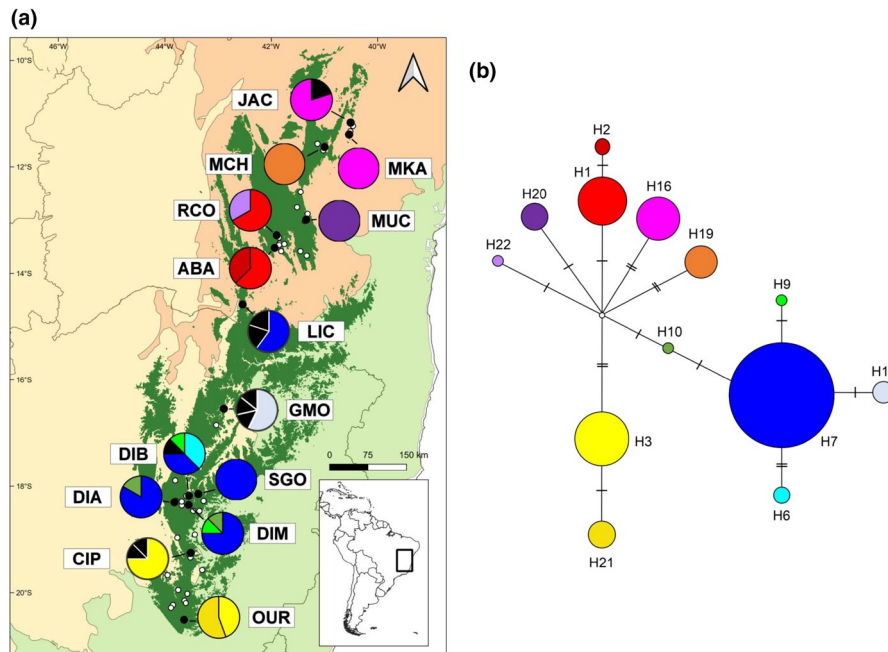
FIGURE 1 (a) Map of the Espinhaço Range (dark green) and its surrounding phytogeographic domains: Caatinga (North, orange), Cerrado (West, beige) and Atlantic Forest (East and South, light green). Dark lines are the Brazilian States borders. This map shows the entire geographic distribution of *Vriesea oligantha*. White points represent occurrence data from herbarium specimens and black points are the sampled populations. The pie charts represent the frequency of occurrence of each haplotype in each population; haplotype colors correspond to those shown in the network; black haplotypes are singletons. (b) Median-joining network depicting the relationships amongst the haplotypes of *V. oligantha*. Population codes: ABA, Abaíra; CIP, Serra do Cipó; DIA, Diamantina (Conselheiro Mata); DIB, Diamantina (Biribiri); DIM, Diamantina (Milho Verde); GMO, Grão Mogol; JAC, Jacobina; LIC, Licínio de Almeida; MCH, Morro do Chapéu; MKA, Miguel Calmón; MUC, Mucugê; OUR, Ouro Branco; RCO, Rio de Contas; SGO, São Gonçalo do Rio Preto

permutations between groups. AMOVA analyses were implemented on ARLEQUIN 3.5.

Recent migration events were estimated in BAYESASS 3.04 (Wilson & Rannala, 2003). Samples were run for 1.0×10^8 interactions with a 10% burn-in, sampling every 1000 interactions. Ancient migration events were estimated using MCMC and coalescence theory approach, implemented in MIGRATE 4.4.3 (Beerli & Felsenstein, 2001), testing two models, using the four phylogenetic lineages as groups: a panmictic model and a neighbour-only model, where migration was only allowed between adjacent groups. For both models, we used a Brownian motion model of mutation under the maximum-likelihood framework and 10 replicates of 1,000,000 runs with a 10% burn-in. Both recent and ancient migration events were estimated using nrSSR.

2.6 | Paleodistribution and ancestral population connections

To predict the current and paleodistributions (i.e. Mid-Holocene, MH, 6 kyr; Last Glacial Maximum, LGM, 21 kyr; and Last Interglacial Maximum, LIG, 120–140 kyr) of *V. oligantha*, we conducted species distribution modelling (SDMs) based on 55 unique occurrence records using an ensemble approach that combined the results from

six distinct modelling algorithms (see Appendix S1 for detailed analyses). From the estimated SDMs, we generated population connectivity maps by summing the least-cost path (LCP) amongst all populations (Chan et al., 2011) to investigate ancestral suitable connections. We created a Friction Layer by inverting the SDM to a dispersal cost layer on ArcMap 10.5 (ESRI, 2016). Next, we calculated corridors that minimise the cost of dispersal between populations by following paths of lowest frictions. To do so, we used the 'Least-Cost Corridors and Paths > Pairwise: All Sites' tool from SDMtoolbox 1.1a (Brown, 2014), implemented on ArcMap 10.5.

2.7 | Demographic reconstruction

To evaluate the demographic history of *V. oligantha*, we used the cpDNA data to calculate the Fu's Fs, Taijma's D and Rozas' R2 statistics and tested their departures from neutrality based on 100,000 coalescent simulations with DnaSP (Librado & Rozas, 2009). We also inferred changes in the species' effective population size through time using an approximate Bayesian computation approach (ABC), implemented in 'abc' (Csilléry et al., 2012) and 'pipemaster' packages (Gehara et al., 2017), both in R 3.6.2 (R Core Team, 2019). Briefly, we simulated genetic data based on three distinct demographic models: expansion, contraction and constant population size, using broad

prior distributions of parameters. The simulated data followed the same number of individuals and sequence length of the lineages estimated by our phylogenetic analysis. The Northern Espinhaço lineage encompassed less than 10 individuals and was not analyzed to avoid bias in our subsequent analyses (Gehara et al., 2017). Then, we generated a group of summary statistics that are dependent on population size and demographic history, evaluating the fit of the simulations to our observed data using a principal component analysis (PCA) on the summary statistics. Finally, we conducted an ABC model selection to evaluate which of the simulated models best fit our observed data. The detailed methods and parametrizations are available in Appendix S2.

2.8 | Roles of climate and geography on population structure

We implemented a Bayesian generaliszed linear mixed modelling (GLMM) approach to test whether population genetic structure of *V. oligantha* is driven by isolation by environment (i.e. temperature and precipitation) and/or isolation by distance models. Refer to Appendix S3 for a detailed method.

3 | RESULTS

3.1 | Phylogenetic inferences and divergence times

The topology of the time-calibrated tree of Tillandsioideae indicates that the *V. oligantha* complex is monophyletic (posterior probability, pp = 1.00) and belongs to Vrieseinae subtribe (Figures S4.1 and S4.2 and Table S5.1). The estimated time to the most recent common ancestor (MRCA) of *V. oligantha* was dated at 3.26 Myr (95% HPD =4.48–1.83 Myr) (Figure 2a and Table S5.1). The phylogenetic analysis revealed four lineages in distinct geographic regions of the Espinhaço Range (Figure 2a and Figure S4.3). The older clade estimated (pp = 1.00; 1.10 Myr, 95% HPD = 1.17–1.04 Myr), was Chapada Diamantina, which includes the MCH, MUC, RCO and ABA populations. Secondly, Diamantina Plateau clade included the GMO, DIB, DIA, DIM, SGO and LIC populations (pp = 0.98, 0.861 Myr, 95% HPD = 1.06–0.494 Myr). Thirdly, the Southern Espinhaço clade comprehended CIP and OUR populations (pp = 0.99, 0.708 Myr, 95% HPD = 0.999–0.274 Myr). Lastly, the youngest clade was the Northern Espinhaço (pp = 0.86, 0.702 Myr, 95% HPD = 1.47–0.076 Myr) and included the most septentrional populations, JAC and MKA populations.
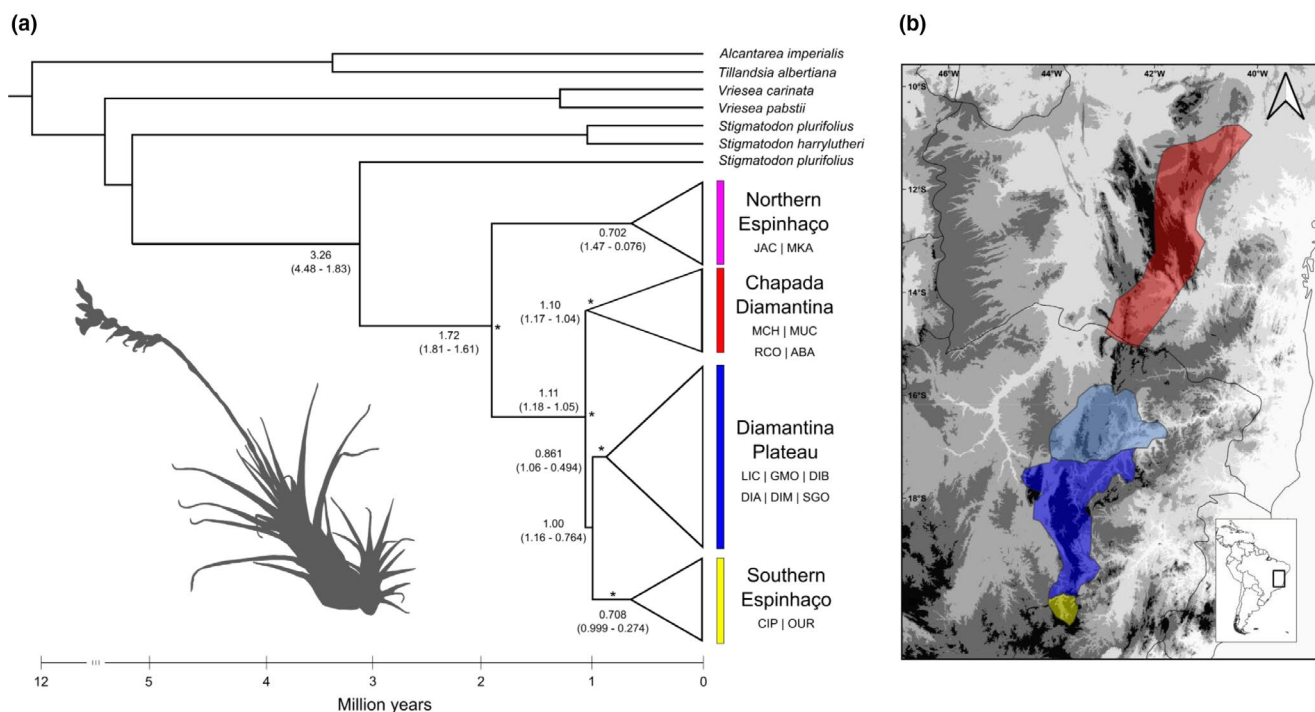

FIGURE 2 (a) Maximum clade credibility tree of *Vriesea oligantha*, depicting four lineages: Northern Espinhaço, Chapada Diamantina, Diamantina Plateau and Southern Espinhaço. Bayesian posterior probabilities higher than 95% are represented by asterisks in each node; mean clade ages (in million years) are written next to each node; values in parentheses are the 95% highest posterior density (HPD). A silhouette of *V. oligantha* is in the inset. (b) The Espinhaço Range bioregionalization proposed by Colli-Silva et al. (2019) is constituted of two provinces, Chapada Diamantina (red) and the Southern Espinhaço, which is subdivided in three districts: Grão-Mogol (light blue), Diamantina Plateau (dark blue) and the Iron Quadrangle (yellow). The elevation gradient is represented by a grey scale, from lower (light) to higher (dark) altitudinal levels. Population codes: ABA, Abaíra; CIP, Serra do Cipó; DIA, Diamantina (Conselheiro Mata); DIB, Diamantina (Biribiri); DIM, Diamantina (Milho Verde); GMO, Grão Mogol; JAC, Jacobina; LIC, Licínio de Almeida; MCH, Morro do Chapéu; MKA, Miguel Calmón; MUC, Mucugê; OUR, Ouro Branco; RCO, Rio de Contas; SGO, São Gonçalo do Rio Preto

3.2 | Genetic diversity

The final alignment matrix with consensus cpDNA sequences of *V. oligantha* had 2065 bp (*trnLF-trnF*, 753 bp and *ycf1*, 1,312 bp), showing 17 polymorphic sites and 22 haplotypes (Figure 1). The haplotype diversity per population ranged from zero to 0.785 and the nucleotide diversity from zero to 0.000761, with an overall haplotype and nucleotide diversity of 0.392 and 0.000280, respectively (Table 2). Few haplotypes are shared amongst populations, but the most frequent haplotype (H7) was found in five populations of the Diamantina Plateau clade, which also showed the highest values of nucleotide and haplotype diversity (Figure 1 and Table 2).

From the nrSSR, we found a total of 162 alleles across loci and 67 were exclusive to single populations. Populations JAC and MUC presented the highest number of private alleles with 16 and 13 alleles, respectively (Table 2). Populations of *V. oligantha* showed an averaged allelic richness ranging from 1.713 to 3.124, whereas variance in allele size ranged from 2.975 to 22.585 (Table 2). Observed and expected heterozygosity per population varied from 0.034 to 0.550 and 0.266 to 0.627, respectively. The mean inbreeding coefficient (F_{IS}) was high and significant for most populations, except for LIC population ranging from 0.125 in DIB and 0.888 in MCH (Table 2).

3.3 | Population structure

BAPS results, based on cpDNA markers, indicated six clusters amongst populations of *V. oligantha* (Figure 3a and Table S5.9). Northern populations (JAC and MKA) are grouped in a cluster, whilst populations from Chapada Diamantina (ABA, MUC and RCO) are clustered together, with exception of MCH, which constitutes a unique group. Diamantina Plateau populations (DIB, DIA, DIM, LIC and SGO) belong to a separate cluster whilst GMO and three individuals of DIB are assembled into a single cluster. The Southern Espinhaço populations (CIP and OUR) form the sixth genetic cluster. STRUCTURE clustering analysis (Figure 3b and Table S5.7), based on nrSSR, revealed a large number of genetic clusters amongst all populations (*K* = 11).

The pairwise F_{ST} values amongst populations were mostly significant, ranging from 0.117 to 1.000 for cpDNA data and from 0.007 to 0.794 for nrSSR data, indicating a widely heterogeneous structure between populations (Figure S4.5 and Tables S5.2 and S5.3). AMOVA showed high values of structure for both markers (cpDNA, F_{ST} = 0.822; nrSSR, F_{ST} = 0.432). When considering a higher hierarchical level (i.e. phylogenetic lineages), AMOVA for cpDNA also showed that the largest proportion of variance was confined amongst populations (F_{ST} = 0.853, $p < 0.001$) (Table 3).

Gene flow estimation from BAYESASS showed few contemporary migration events, only amongst nearby populations (Table S5.4).

TABLE 2 Genetic diversity and tests of neutrality of 14 populations of *Vriesea oligantha*

Pop	Plastidial								Nuclear							
	Haplotypes	p	Hd	ss	Fu	D	R2	P	A	A_P	R	Var	H_O	H_E	F_{IS}
JAC	H15–H16	0.000194	0.400	1	0.090	−0.816	0.400	100	50	16	3.014	21.839	0.486	0.556	0.182[a]
MKA	H16	0	0	0	0	0	0	—	—	—	—	—	—	—	—
MCH	H19	0	0	0	0	0	0	66.7	19	5	1.725	2.975	0.034	0.288	0.888[a]
MUC	H20	0	0	0	0	0	0	100	53	13	3.124	17.813	0.471	0.627	0.281[a]
RCO	H1, H22	0.000517	0.533	2	1.723	1.031	0.266	66.7	21	0	1.713	3.694	0.181	0.266	0.357[a]
ABA	H1–H2	0.000259	0.535	1	0.866	1.166	0.267	88.9	36	7	2.248	13.705	0.147	0.444	0.679[a]
LIC	H7, H17–H18	0.000581	0.7	3	−0.185	−1.048	0.266	77.8	20	3	2.084	22.585	0.519	0.377	−0.258
GMO	H11–H14	0.000484	0.714	2	−1.483*	0.927	0.250	77.8	32	2	1.980	6.389	0.219	0.322	0.343[a]
DIB	H6–H9	0.000761	0.785	4	−0.328	0.081	0.172	100	59	3	3.111	13.687	0.550	0.609	0.125[a]
DIA	H7, H10	0.000161	0.333	1	−0.002	−0.933	0.372	100	51	8	3.043	14.433	0.350	0.592	0.441[a]
DIM	H7, H9–H10	0.000242	0.464	2	−0.998	−1.310	0.216	—	—	—	—	—	—	—	—
SGO	H7	0	0	0	0	0	0	88.9	41	3	2.718	10.507	0.361	0.510	0.325[a]
CIP	H3–H5	0.00045	0.464	3	0.071	−0.812	0.161*	88.9	32	3	2.251	12.496	0.145	0.430	0.676[a]
OUR	H3, H21	0.000269	0.555	1	1.015	1.401	0.277	55.6	23	4	1.773	9.245	0.071	0.291	0.766[a]

Abbreviations: A, number of alleles; A_P, number of private alleles; D, Tajimas's D statistics; F_{IS}, Inbreeding coefficient; Fu, Fu's Fs statistics; *Hd*, haplotype diversity; H_E, Expected heterozygosity; H_O, Observed heterozygosity; p, nucleotide diversity; P, percentage of polymorphic loci; R, allelic richness; R2, Ramos-Onsins-Rozas' statistics; *ss*, polymorphic sites; Var, variance in allele size.

[a]Departures of within-population inbreeding coefficients from Hardy–Weinberg equilibrium (*p*-value < 0.01).
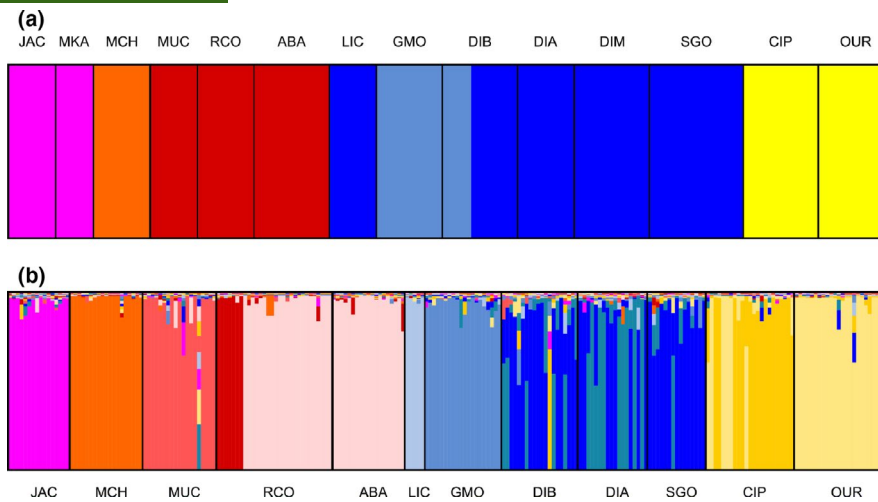
*p-value < 0.01.

FIGURE 3 Clustering methods used for *Vriesea oligantha* populations based on (a) cpDNA, using BAPS, depicting six clusters and (b) nrSSR, using STRUCTURE software, depicting eleven clusters. In all plots, each color represents a given cluster. Population codes: ABA, Abaíra; CIP, Serra do Cipó; DIA, Diamantina (Conselheiro Mata); DIB, Diamantina (Biribiri); DIM, Diamantina (Milho Verde); GMO, Grão Mogol; JAC, Jacobina; LIC, Licínio de Almeida; MCH, Morro do Chapéu; MKA, Miguel Calmón; MUC, Mucugê; OUR, Ouro Branco; RCO, Rio de Contas; SGO, São Gonçalo do Rio Preto

TABLE 3 Analysis of molecular variance on cpDNA sequences and nrSSR, based on the phylogenetic lineages

Clustering method	Source of variation	df	Sum of Squares	Variance components	Variation (%)	F-statistics
cpDNA						
All populations	Amongst populations	13	125.787	1.38841	82.2	$F_{ST} = 0.822$
	Within populations	81	24.297	0.29997	17.7	
	Amongst lineages	3	95.702	1.35333	65.9	$F_{CT} = 0.659$
Phylogenetic lineages	Amongst populations within lineages	10	30.085	0.39953	19.4	$F_{SC} = 0.571$
	Within populations	81	24.297	0.29997	14.6	$F_{ST} = 0.853$
	Total	94	150.084	2.05283	100	
nrSSR						
All populations	Amongst populations	11	302.447	0.70207	43.2	$F_{ST} = 0.432$
	Within populations	446	410.732	0.92092	56.7	
	Total	457	88079.555	238.4214	100	

All values of *F*-statistics are significant (*p*-value < 0.001).

Similarly, MIGRATE estimated few ancient migration events between neighbouring populations (Figure S4.4 and Table S5.5), where the migration only between adjacent groups model was better supported than the panmictic model (Table S5.6).

3.4 | Palaeoclimatic distribution and ancestral population connections

Our SDMs indicated that between 120 and 140 kyr ago (LIG), high suitable areas for *V. oligantha* were concentrated in sparse fragments, southwards from the current distribution, although midsuitability would be observed all over the Espinhaço Range. Later, as the climate got colder, during the LGM (21 kyr), suitable areas of *V. oligantha* might have

increased, becoming progressively connected (Figure 4c). According to our SDMs, the *V. oligantha's* distribution became more fragmented once again during the Mid-Holocene (6 kyr), with suitable areas in the Northern Espinhaço (Figure 4b). The current distribution mainly reflects areas of high altitude in the Espinhaço Range (Figure 4a).

Analysis of the LCP across isolated populations revealed suitable areas of ancestral connection over all investigated periods, especially between the Chapada Diamantina and the Diamantina Plateau populations (Figure 5). However, those connections seem broader in the LIG (Figure 5d), while they become progressively narrow until the current climate conditions, with high suitability amongst populations in the Diamantina Plateau (Figure 5a–c). Populations from the northern and southern peripheries of the distribution presented lower connections with the central groups in all periods.

FIGURE 4 Ensemble distribution models for *Vriesea oligantha* under (a) Current, (b) Mid-Holocene (6 kyr), (c) Last Glacial Maximum (21 kyr) and (d) Last Interglacial Maximum (120 kyr) climatic conditions. The thin line represents the current delimitation of the Espinhaço Range
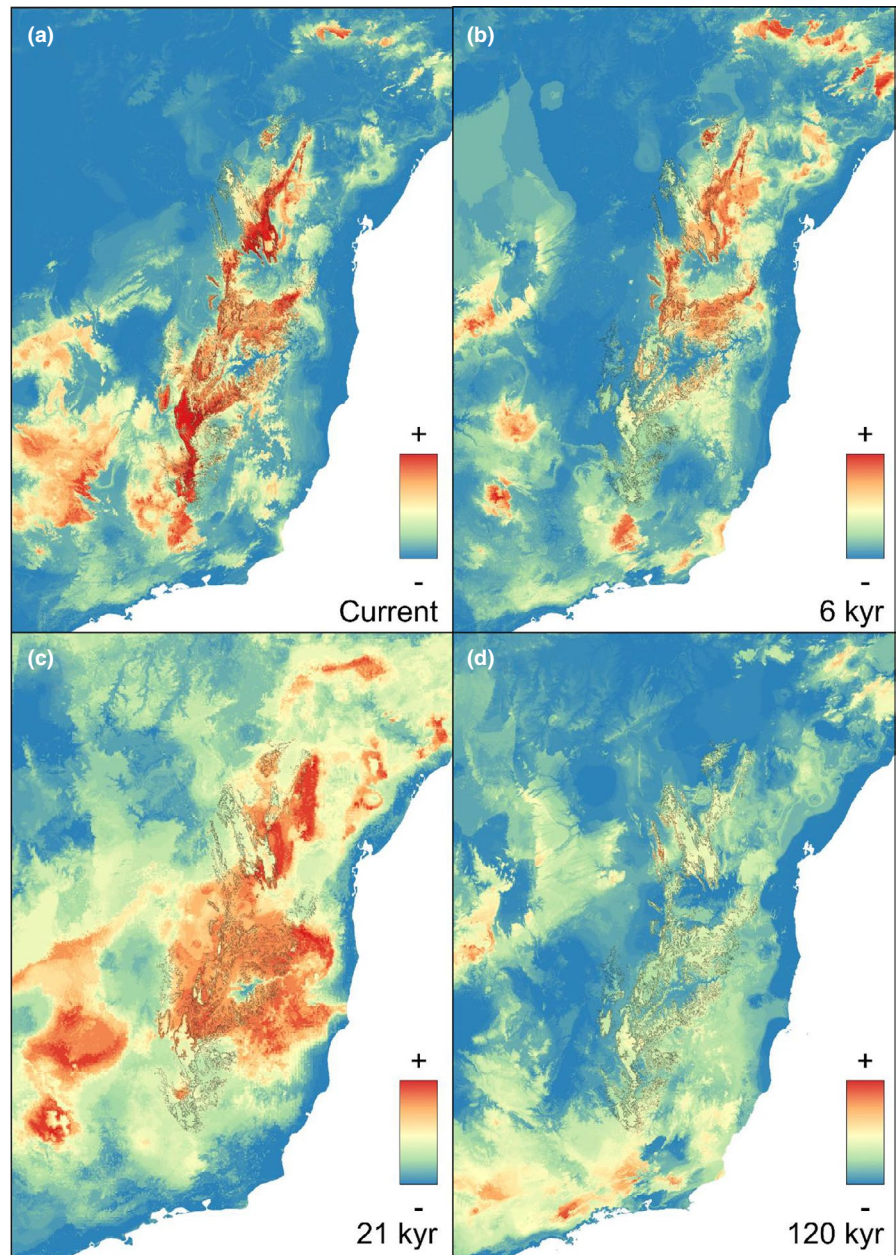
3.5 | Demographic analyses

All populations exhibited no departure from neutrality on demographic analyses, except for GMO (in Fu's FS) and CIP (in Roza's R2) (Table 2). From our ABC analysis, all analyzed lineages fitted within the simulate data, as observed by the PCA (Figure S4.6). The expansion model was consistently supported as the most likely of the three demographic models for all three lineages analyzed. The probability of expansion was ≥60%, and the probability of the other models was ≤34% for all analyzed lineages (Table S5.8).

3.6 | Relative roles of climate and geography

Our GLMM analysis indicated that environmental and geographical distances are both good predictors of genetic variation in *V.*

oligantha. Contrasted with other predictors, the model including a combination of both isolation by geographic distance (IBD) and by environment (IBE) had the best model fit as indicated by DIC (Deviance Information Criterion) for both plastidial and nuclear genomes (Table 4).

4 | DISCUSSION

4.1 | Geographic and environmental isolation are the main drivers of population divergence in *Vriesea oligantha*

The divergence age between *V. oligantha* and its outgroup dates back to the Pliocene-Pleistocene transition (3.26 Myr; Figure 2a), mirroring previous phylogenetic analyses (Kessous et al., 2019; Machado
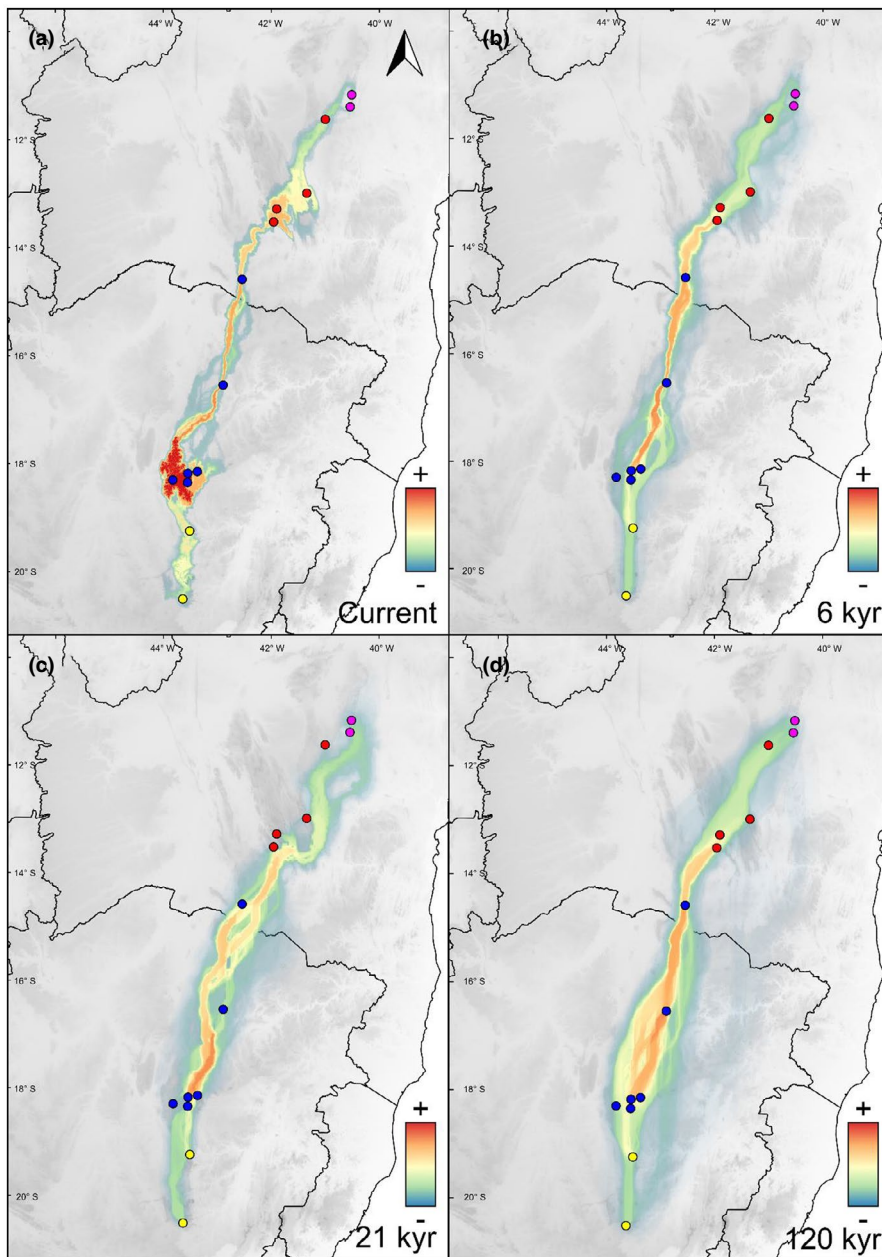
FIGURE 5 Potential dispersal corridors between *Vriesea oligantha* populations based on friction layers throughout the Espinhaço Range, across four period times. (a) Current; (b) Mid-Holocene (6 kyr); (c) Last Glacial Maximum (21 kyr); and (d) Last Interglacial Maximum (120 kyr). Each color within circles represents a lineage from the phylogenetic tree—pink, Northern Espinhaço; red, Chapada Diamantina; blue, Diamantina Plateau; yellow, Southern Espinhaço. The elevation gradient is represented by a grey scale, from lower (light) to higher (dark) altitudinal levels

TABLE 4 Results of generalised linear mixed models (GLMM) testing the influence of geographic distance and climatic differences, based on 19 bioclimatic variables, on the genetic divergence amongst populations of *Vriesea oligantha*

	cpDNA			nrSSR		
Model	**DIC**	**ΔDIC**	**DIC weight**	**DIC**	**ΔDIC**	**DIC weight**
Null	810.1204	9.6164	0.0077	113.2596	9.5066	0.0045
Geography	811.7689	11.2648	0.0034	106.2901	2.5372	0.1461
Climate	806.3522	5.8482	0.0504	**103.7529**	**<0.001**	**0.5196**
Geography + Climate	**800.5041**	**<0.001**	**0.9386**	104.6625	0.9096	0.3297

The best model for each data set is highlighted in bold.

Abbreviation: DIC, deviance information criterion.

et al., 2020). This period is marked by a decrease in global temperature and the beginning of glaciations in the Northern Hemisphere (Prell, 1984). In this context, *V. oligantha* is a remarkable model to test the effects of climatic oscillations over the biological community, since this species originated in the early-Pleistocene, prevailing over several cycles of climatic fluctuations until today.

Our results showed that the intraspecific divergence events of *V. oligantha* are older than those associated with the latest Pleistocene climatic oscillations, thus cannot be explained solely by the late-Quaternary refugia hypothesis (Haffer, 1969; Rull, 2011). Moreover, extreme amplitude in climatic fluctuations was remarkable events in the mid-Pleistocene (Lisiecki & Raymo, 2007), when *V. oligantha* lineages diversified (Figure 2). This supports the view that climate fluctuations that occurred along the whole Quaternary are key components for understanding population differentiation processes due to the flickering connectivity amongst populations that led to the species-pump mechanism. Altogether, these findings reinforce the importance of climate changes throughout the whole Pleistocene in the diversification of the montane biota in the Neotropics (Antonelli et al., 2018; Perrigo et al., 2020; Silva et al., 2018; Vasconcelos et al., 2020). Accordingly, diversification events throughout the Quaternary are congruent amongst many extant lineages from distinct Neotropical montane formations, as in the Espinhaço itself (e.g. Barres et al., 2019; Bonatelli et al., 2014; Chaves et al., 2019; Nascimento et al., 2018; Vasconcelos et al., 2020); Serra do Mar and Mantiqueira mountains (Mota et al., 2020); the páramos (e.g. Hughes & Atchison, 2015; Madriñán et al., 2013) and the pantepuis (e.g. Rull & Vegas-Vilarrúbia, 2020; Salerno et al., 2012), although the role of species pump in these latter remain to be tested.

Populations of *V. oligantha* are genetically differentiated by a combined interplay of both geographic distances and environmental differences, as expected under the IBD and IBE models, respectively (Table 4). These results suggest that climatic variables along the Espinhaço Range were determinant predictors of the genetic structure of the populations of *V. oligantha*. In fact, climate along the Espinhaço Range is quite heterogeneous (Giulietti et al., 1987) (Table 4). For instance, the Northern Espinhaço climate is markedly drier and hotter, with long periods of low (or even absence of) precipitation while the climate of the mid-south Espinhaço has milder temperatures and higher humidity levels (Giulietti et al., 1987; Zappi et al., 2003). Such climatic variation has the potential to rapidly influence evolution by triggering ecological divergence (Campbell & Powers, 2015), especially in a scenario with reduced interpopulation gene flow as observed in *V. oligantha* (Figure 3 and Figure S4.4). In fact, the four phylogeographic lineages (Figure 2) present some anatomical and morphological differences (Silva et al., 2020) that might be associated with adaptive responses to environmental factors.

Our ABC demographic analyses showed that most lineages of *V. oligantha* presented a demographic expansion over the LGM (Table S5.8), depicting a major spatial reorganization of this species during a colder climate. The expansion and the consequential population contractions towards the present might have promoted connections and disconnections amongst adjacent populations. Similarly, the SDMs using extant and past climatic variables revealed middle to lower suitability during warmer periods (current; mid-holocene: 6 kyr, and LIG: 120–140 kyr)

when populations of *V. oligantha* might have survived in sparse fragment of small areas of its distribution (Figure 4). As expected, during the LGM (21 kyr), the colder climate might have promoted the increase of suitable habitats and populations might have become more connected (Figure 4). Despite these differences due to past climatic variations, suitable areas of ancestral connections amongst populations were present allover investigated periods, which might have allowed eventual migrations, at least amongst core populations (i.e Diamantina Plateau populations—Figure 5). In agreement, MIGRATE analysis revealed that gene flow amongst populations was limited to adjacent populations (Figure S4.4 and Tables S5.5 and S5.6). Therefore, we expect the impacts of Pleistocene climate changes on *V. oligantha* populations differentiation to be associated with local persistence during multiple cycles of demographic expansion and contraction. Demographic dynamics estimated by our ABC analyses and the SDMs are in agreement with the postulated species-pump mechanism in the divergence of intraspecific lineages of *V. oligantha* and possible to other endemic lineages of the Espinhaço Range. Accordingly, paleopalinological studies in the Espinhaço area have also showed herbaceous vegetation turnover in the last thousand years (Behling, 2002; de Barros et al., 2011; Horák-Terra et al., 2015), concurring with the flickering connectivity effect in the Espinhaço Range.

Together with climatic differences, the other important predictor of *V. oligantha* population differentiation was geographic distances, as expected in IBD model (Table 4). In general, most populations of *V. oligantha* had extremely low gene flow amongst each other, with only a few connected adjacent populations (Figure S4.5 and Tables S5.2 and S5.3). In fact, restricted population connectivity has been reported for several naturally fragmented habitats, especially in mountain systems (e.g. Mota et al., 2020; Muellner-Riehl et al., 2019). Such limited gene flow amongst populations suggests that both pollen and seed dispersal might be restricted. Since maternal inheritance of plastidial DNA and biparental inheritance of nuclear DNA are the most common pattern for Angiosperms (Ennos, 1994), the genetic differentiation results indicate that gene flow via seeds is comparatively less efficient than via pollen, as noticed by the much higher genetic structure of cpDNA (F_{ST} = 0.82, Table 3 and Figure S4.5) than nrSSR (F_{ST} = 0.43, Table 3 and Figure S4.5). The discrepancy between the two genomes may indicate the role of pollinators in maintaining a relative cohesion between close populations, since seeds are poorly dispersed, a common trend in other plant lineages of the Espinhaço Range (Silveira et al., 2020). However, it is important to notice that both coalescent and Bayesian analysis revealed limited nuclear migration rates amongst populations (Tables S5.4 and S5.5) suggesting a restricted dispersal even via pollen. Future investigations on specific and effective pollinators and their foraging behaviours may help us to understand their role in connectivity and population differentiation of *V. oligantha* in such naturally fragmented habitats.

4.2 | Phylogeography of *Vriesea oligantha*: insights from micro to macroevolution in the Espinhaço Range

The phylogeographic results of *V. oligantha* showed a remarkable congruence between the population genetic structure and the bioregionalization proposed by Colli-Silva et al. (2019), based on patterns of plant endemism in the Espinhaço Range (Figure 2). Similar biogeographic patterns were also pointed out by several other studies using floristic and faunistic composition, as well as endemicity indexes (e.g. Bitencourt & Rapini, 2013; Bünger et al., 2014; Campos et al., 2019; Chaves et al., 2015) and phylogenetic histories (e.g. Chaves et al., 2019; Ribeiro et al., 2014). These results not only suggest that evolutionary history and community assembling of distinct areas in the Espinhaço Range (Zappi et al., 2017) might be under the same influence of climatic oscillations and spatial connectivity but also imply that population differentiation and macroevolutionary diversification should be linked over a deep evolutionary time.

Both Northern Espinhaço and Chapada Diamantina lineages and their clustering analyses support the congruence with the Chapada Diamantina province (Colli-Silva et al., 2019). Populations from the Diamantina Plateau clade mainly match the Diamantina Plateau district, though the GMO population is a noteworthy exception. As evidenced by the clustering analysis (BAPS and STRUCTURE—Figure 3 and Tables S5.7 and S5.9), GMO remained distinct as a single cluster, unarguably fitting into the Grão-Mogol district (Colli-Silva et al., 2019). The particularity of this district has already been reported elsewhere (e.g. Echternacht et al., 2011; Pirani et al., 2003). Its environmental discontinuity might be a factor leading to the singularity of these mountains, since they are an ecotone between the *Cerrado* and *Caatinga* domains, possibly affecting the dynamics of the biological community of this region and resulting in a particular evolutionary history.

The fourth estimated clade, the Southern Espinhaço, includes CIP and OUR populations, the latter coinciding with the Iron Quadrangle district, the southernmost bioregion of the Espinhaço Range (Colli-Silva et al., 2019). However, we could not directly link this clade with the Iron Quadrangle district, since its diagnostic characteristic is the presence of ironstone outcrops, while CIP and OUR are associated with quartzitic soils (Saadi, 1995). Despite the soil differences, the relative geographic proximity of CIP and OUR with the Iron Quadrangle district may promote the divergence of the Southern Espinhaço clade due to biotic interactions and constraints fostered by the singular environment and community of the Iron Quadrangle (Jacobi et al., 2007; Zappi et al., 2017). Further analyses exploring the role of ecological interactions and how they affect speciation amongst communities could improve this hypothesis (Johnson & Stinchcombe, 2007).

The evolution of species-rich biotas is remarkably known for its complex drivers (Antonelli et al., 2018; Rull, 2011), and other triggers might also help understanding the intraspecific lineage diversification of organisms from montane systems worldwide, such as pollination strategies (Franceschinelli et al., 2006), niche conservatism (de Mattos et al., 2019) and edaphic adaptations to heterogeneous topography (Alcantara et al., 2018). Major tectonic events in the Espinhaço Range far precede many of the angiosperm intraspecific differentiation (Dussin & Dussin, 1995; Magalhães Junior et al., 2015; Vasconcelos et al., 2020), and erosion rates are much lower in this region than in tectonically active mountainous areas, such as Himalayas, Alps and Northern Andes (Herman et al., 2013), suggesting the Pleistocene climatic fluctuation effects on biodiversity diversification as more relevant than those geological processes. Still, neotectonic events could play a role in the dynamics of microevolutionary processes that have shaped the current macroevolutionary patterns of the Espinhaço biota. For instance, the fluvial dynamics in the region was intense over all Pleistocene, resulting in fluvial dissection and shaping valleys that led to the formation of flood plains constituted mainly by sediments derived from quartzite soils (Magalhães Junior et al., 2015; Saadi, 1995). Such dynamics could influence the species-pump dynamics by, for example, preventing the contact of populations due to ancient river barriers. Despite the link between geological evolution and species diversification is still growing, new approaches connecting both subjects, such as the 'geogenomics' (Baker et al., 2014) or the 'mountain-geobiodiversity' (Muellner-Riehl et al., 2019), are emerging fields with exciting discoveries, combining genomic, climatic and geological data in order to elucidate the processes that influenced evolution in these areas (Antonelli et al., 2018). Such approaches could, in fact, shed light on recent discussions about mountain evolution and the possible older divergence events masked by extinctions during Pleistocene climatic changes (Perrigo et al., 2020). In the future, the relative role of the microevolutionary processes could be tested by incorporating association analyses of the entire or partial genomes from multiple species with climatic, geological, geophysical, geochronological and functional ecological datasets under a comparative framework.

4.3 | Microevolutionary processes as a proxy for understanding macroevolutionary patterns

We showed that microevolutionary processes underlying the phylogeographic patterns of *V. oligantha* are a consequence of IBD and IBE throughout its distribution. This suggests continuous cycles of climate changes in the Pleistocene might be a key for understanding evolutionary responses (speciation, extinction, migration and adaptation) due to the flickering connectivity amongst populations that led to the species-pump mechanism. Considering the assumption that population differentiation is the basic mechanism of speciation, the concordant patterns between the divergence amongst lineages within the *V. oligantha* complex and the Espinhaço Range biogeography generate powerful insights into how climatic variables and limited gene flow might have shaped early stages of macroevolutionary patterns. Despite the long-standing debate in biogeography about whether correlation between congruence in time and space would be sufficient to yield causation (Perrigo et al., 2020), our study attempts to fill the gap between microevolutionary and macroevolutionary scales, a necessary approach to pave the way on the initial effects

of population differentiation that ultimately lead to the origin of new species and spatial patterns of biodiversity distribution. Additional evidence using distinct organisms could also provide contrasting examples of how microevolutionary processes act and translate into the current biogeographic patterns of tropical montane biotas.

ORCID

Marcos Vinicius Dantas-Queiroz 🄳 https://orcid.org/0000-0002-5444-8121
Tami da Costa Cacossi 🄳 https://orcid.org/0000-0001-6245-1382
Bárbara Simões Santos Leal 🄳 https://orcid.org/0000-0003-4401-3252
Cleber Juliano Neves Chaves 🄳 https://orcid.org/0000-0002-5960-7304
Thais N. C. Vasconcelos 🄳 https://orcid.org/0000-0001-9991-7924
Leonardo de Melo Versieux 🄳 https://orcid.org/0000-0003-1560-3691
Clarisse Palma-Silva 🄳 https://orcid.org/0000-0003-0192-5489

REFERENCES

Acuña Castillo, R., Luebert, F., Henning, T., & Weigend, M. (2019). Major lineages of Loasaceae subfam. Loasoideae diversified during the Andean uplift. *Molecular Phylogenetics and Evolution*, *141*, 106616. https://doi.org/10.1016/j.ympev.2019.106616

Alcantara, S., Ree, R. H., & Mello-Silva, R. (2018). Accelerated diversification and functional trait evolution in Velloziaceae reveal new insights into the origins of the campos rupestres' exceptional floristic richness. *Annals of Botany*, *122*(1), 1–16. https://doi.org/10.1093/aob/mcy063

Antonelli, A., Kissling, W. D., Flantua, S. G. A., Bermúdez, M. A., Mulch, A., Muellner-Riehl, A. N., Kreft, H., Linder, H. P., Badgley, C., Fjeldså, J., Fritz, S. A., Rahbek, C., Herman, F., Hooghiemstra, H., & Hoorn, C. (2018). Geological and climatic influences on mountain biodiversity. *Nature Geoscience*, *11*(10), 718–725. https://doi.org/10.1038/s41561-018-0236-z

Arnaud-Haond, S., & Belkhir, K. (2006). GENCLONE: A computer program to analyse genotypic data, test for clonality and describe spatial clonal organization. *Molecular Ecology Notes*, *7*(1), 15–17. https://doi.org/10.1111/j.1471-8286.2006.01522.x

Baker, P. A., Fritz, S. C., Dick, C. W., Eckert, A. J., Horton, B. K., Manzoni, S., Ribas, C. C., Garzione, C. N., & Battisti, D. S. (2014). The emerging field of geogenomics: Constraining geological problems with genetic data. *Earth-Science Reviews*, *135*, 38–47. https://doi.org/10.1016/j.earscirev.2014.04.001

Bandelt, H. J., Forster, P., & Rohl, A. (1999). Median-joining networks for inferring intraspecific phylogenies. *Molecular Biology and Evolution*, *16*(1), 37–48. https://doi.org/10.1093/oxfordjournals.molbev.a026036

Barfuss, M. H. J., Samuel, R., Till, W., & Stuessy, T. F. (2005). Phylogenetic relationships in subfamily Tillandsioideae (Bromeliaceae) based on DNA sequence data from seven plastid regions. *American Journal of Botany*, *92*(2), 337–351. https://doi.org/10.3732/ajb.92.2.337

Barfuss, M. H., Till, W., Leme, E. M., Pinzón, J. P., Manzanares, J. M., Halbritter, H., Samuel, R., & Brown, G. K. (2016). Taxonomic revision of Bromeliaceae subfam. Tillandsioideae based on a multilocus DNA sequence phylogeny and morphology. *Phytotaxa*, *279*(1), 1–97.

Barres, L., Batalha-Filho, H., Schnadelbach, A. S., & Roque, N. (2019). Pleistocene climatic changes drove dispersal and isolation of *Richterago discoidea* (Asteraceae), an endemic plant of campos rupestres in the central and eastern Brazilian sky islands. *Botanical Journal of the Linnean Society*, *189*(2), 132–152.

Beerli, P., & Felsenstein, J. (2001). Maximum likelihood estimation of a migration matrix and effective population sizes in n subpopulations by using a coalescent approach. *Proceedings of the National Academy of Sciences of the United States of America*, *98*(8), 4563–4568. https://doi.org/10.1073/pnas.081068098

Behling, H. (2002). South and southeast Brazilian grassland during Late Quaternary times: A synthesis. *Palaeogeography, Palaeoclimatology, Palaeoecology*, *177*(1–2), 19–27.

Bitencourt, C., & Rapini, A. (2013). Centres of endemism in the Espinhaço Range: Identifying cradles and museums of Asclepiadoideae (Apocynaceae). *Systematics and Biodiversity*, *11*(4), 525–536. https://doi.org/10.1080/14772000.2013.865681

Bonatelli, I. S., Perez, M. F., Peterson, A. T., Taylor, N. P., Zappi, D. C., Machado, M. C., & Moraes, E. M. (2014). Interglacial microrefugia and diversification of a cactus species complex: Phylogeography and palaeodistributional reconstructions for *Pilosocereus aurisetus* and allies. *Molecular Ecology*, *23*(12), 3044–3063.

Brown, J. L. (2014). SDMtoolbox: A python-based GIS toolkit for landscape genetic, biogeographic and species distribution model analyses. *Methods in Ecology and Evolution*, *5*(7), 694–700. https://doi.org/10.1111/2041-210X.12200

Bünger, M. D. O., Stehmann, J. R., & Oliveira-Filho, A. T. (2014). Myrtaceae throughout the Espinhaço Mountain Range of central-eastern Brazil: Floristic relationships and geoclimatic controls. *Acta Botanica Brasilica*, *28*(1), 109–119. https://doi.org/10.1590/S0102-33062014000100011

Cacossi, T., Dantas-Queiroz, M. V., & Palma-Silva, C. (2019). Transferability of nuclear microsatellites markers to *Vriesea oligantha* (Bromeliaceae), an endemic species from Espinhaço Range, Brazil. *Brazilian Journal of Botany*, *42*(4), 727–733. https://doi.org/10.1007/s40415-019-00560-z

Campbell, D. R., & Powers, J. M. (2015). Natural selection on floral morphology can be influenced by climate. *Proceedings of the Royal Society B: Biological Sciences*, *282*(1808), 1–7.

Campos, L., Moro, M. F., Funk, V. A., & Roque, N. (2019). Biogeographical review of Asteraceae in the Espinhaço Mountain Range, Brazil. *The Botanical Review*, *85*(4), 293–336. https://doi.org/10.1007/s12229-019-09216-9

Chan, L. M., Brown, J. L., & Yoder, A. D. (2011). Integrating statistical genetic and geospatial methods brings new power to phylogeography. *Molecular Phylogenetics and Evolution*, *59*(2), 523–537. https://doi.org/10.1016/j.ympev.2011.01.020

Chaves, A. V., Freitas, G. H. S., Vasconcelos, M. F., & Santos, F. R. (2015). Biogeographic patterns, origin and speciation of the endemic birds from eastern Brazilian mountaintops: A review. *Systematics and Biodiversity*, *13*(1), 1–16. https://doi.org/10.1080/14772000.2014.972477

Chaves, A. V., Vasconcelos, M. F., Freitas, G. H. S., & Santos, F. R. (2019). Vicariant events in the montane hummingbird genera *Augastes* and *Schistes* in South America. *Ibis*, *162*(3), 1060–1067. https://doi.org/10.1111/ibi.12777

Colli-Silva, M., Vasconcelos, T. N. C., & Pirani, J. R. (2019). Outstanding plant endemism levels strongly support the recognition of campo rupestre provinces in mountaintops of eastern South America. *Journal of Biogeography*, *46*(8), 1723–1733.

Corander, J., Marttinen, P., Sirén, J., & Tang, J. (2008). Enhanced Bayesian modelling in BAPS software for learning genetic structures of populations. *BMC Bioinformatics*, *9*(1), 539. https://doi.org/10.1186/1471-2105-9-539

Csilléry, K., François, O., & Blum, M. G. (2012). Abc: An R package for approximate Bayesian computation (ABC). *Methods in Ecology and Evolution*, *3*(3), 475–479.

Darriba, D., Taboada, G. L., Doallo, R., & Posada, D. (2012). jModelTest 2: More models, new heuristics and parallel computing. *Nature Methods*, *9*(8), 772. https://doi.org/10.1038/nmeth.2109

de Barros, L. F., Lavarini, C., Lima, L. S., & Magalhães-Júnior, A. P. (2011). Synthesis of the Late-Quaternary paleobioclimatic scenarios in Minas Gerais State/Southeastern Brazil. *Sociedade & Natureza*, *23*(3), 371–385.

de Mattos, J. S., Morellato, L. P. C., Camargo, M. G. G., & Batalha, M. A. (2019). Plant phylogenetic diversity of tropical mountaintop rocky grasslands: Local and regional constraints. *Plant Ecology*, *220*(12), 1119–1129. https://doi.org/10.1007/s11258-019-00982-5

Drummond, A. J., & Rambaut, A. (2007). BEAST: Bayesian evolutionary analysis by sampling trees. *BMC Evolutionary Biology*, *7*(1), 214. https://doi.org/10.1186/1471-2148-7-214

Dussin, I. A., & Dussin, T. M. (1995). Supergrupo Espinhaço: Modelo de evolução geodinâmica. *Geonomos*, *3*(1), 19–26. https://doi.org/10.18285/geonomos.v3i1.212

Earl, D. A., & von Holdt, B. M. (2012). STRUCTURE HARVESTER: A website and program for visualizing STRUCTURE output and implementing the Evanno method. *Conservation Genetics Resources*, *4*(2), 359–361. https://doi.org/10.1007/s12686-011-9548-7

Echternacht, L., Trovó, M., Oliveira, C. T., & Pirani, J. R. (2011). Areas of endemism in the Espinhaço Range in Minas Gerais, Brazil. *Flora*, *206*(9), 782–791. https://doi.org/10.1016/j.flora.2011.04.003

Ennos, R. A. (1994). Estimating the relative rates of pollen and seed migration among plant populations. *Heredity*, *72*(3), 250–259. https://doi.org/10.1038/hdy.1994.35

ESRI. (2016). *ArcGis desktop*. Redlands.

Evanno, G., Regnaut, S., & Goudet, J. (2005). Detecting the number of clusters of individuals using the software STRUCTURE: A simulation study. *Molecular Ecology*, *14*(8), 2611–2620. https://doi.org/10.1111/j.1365-294X.2005.02553.x

Excoffier, L., & Lischer, H. E. L. (2010). Arlequin suite ver. 3.5: A new series of programs to perform population genetics analyses under Linux and Windows. *Molecular Ecology Resources*, *10*(3), 564–567.

Flantua, S. G. A., & Hooghiemstra, H. (2018). Historical connectivity and mountain biodiversity. In C. Hoorn, A. Perrigo, & A. Antonelli (Eds.), *Mountains, Climate and Biodiversity* (pp. 171–185). Wiley-Blackwell.

Flantua, S. G. A., O'Dea, A., Onstein, R. E., Giraldo, C., & Hooghiemstra, H. (2019). The flickering connectivity system of the north Andean páramos. *Journal of Biogeography*, *46*(8), 1808–1825. https://doi.org/10.1111/jbi.13607

Franceschinelli, E. V., Jacobi, C. M., Drummond, M. G., & Resende, M. F. S. (2006). The genetic diversity of two Brazilian *Vellozia* (Velloziaceae) with different patterns of spatial distribution and pollination biology. *Annals of Botany*, *97*(4), 585–592. https://doi.org/10.1093/aob/mcl007

Gehara, M., Garda, A. A., Werneck, F. P., Oliveira, E. F., da Fonseca, E. M., Camurugi, F., Magalhães, F. D. M., Lanna, F. M., Sites, J. W., Marques, R., Silveira-Filho, R., São Pedro, V. A., Colli, G. R., Costa, G. C., & Burbrink, F. T. (2017). Estimating synchronous demographic changes across populations using hABC and its application for a herpetological community from northeastern Brazil. *Molecular Ecology*, *26*(18), 4756–4771. https://doi.org/10.1111/mec.14239

Giulietti, A. M., Menezes, N. L., Pirani, J. R., Meguro, M., & Wanderley, M. G. L. (1987). Flora da Serra do Cipó, Minas Gerais: Caracterização e lista das espécies. *Boletim De Botânica Da Universidade De São Paulo*, *9*, 1–151. https://doi.org/10.11606/issn.2316-9052.v9i0p1-151

Givnish, T. J., Barfuss, M. H. J., Van Ee, B., Riina, R., Schulte, K., Horres, R., Gonsiska, P. A., Jabaily, R. S., Crayn, D. M., Smith, J. A. C., Winter, K., Brown, G. K., Evans, T. M., Holst, B. K., Luther, H., Till, W., Zizka, G., Berry, P. E., & Sytsma, K. J. (2011). Phylogeny, adaptive radiation, and historical biogeography in Bromeliaceae: Insights from an eight-locus plastid phylogeny. *American Journal of Botany*, *98*(5), 872–895. https://doi.org/10.3732/ajb.1000059

Goudet, J. (1995). FSTAT (Version 1.2): A computer program to calculate F-statistics. *Journal of Heredity*, *86*(6), 485–486.

Haffer, J. (1969). Speciation in Amazonian Forest Birds. *Science*, *165*(3889), 131–137.

Haffer, J. (1997). Alternative models of vertebrate speciation in Amazonia: An overview. *Biodiversity & Conservation*, *6*, 451–476.

Herman, F., Seward, D., Valla, P. G., Carter, A., Kohn, B., Willett, S. D., & Ehlers, T. A. (2013). Worldwide acceleration of mountain erosion under a cooling climate. *Nature*, *504*(7480), 423–426.

Horák-Terra, I., Martínez Cortizas, A., da Luz, C. F. P., Rivas López, P., Silva, A. C., & Vidal-Torrado, P. (2015). Holocene climate change in central-eastern Brazil reconstructed using pollen and geochemical records of Pau de Fruta mire (Serra do Espinhaço Meridional, Minas Gerais). *Palaeogeography, Palaeoclimatology, Palaeoecology*, *437*, 117–131. https://doi.org/10.1016/j.palaeo.2015.07.027

Hughes, C. E., & Atchison, G. W. (2015). The ubiquity of alpine plant radiations: From the Andes to the Hengduan Mountains. *New Phytologist*, *207*(2), 275–282. https://doi.org/10.1111/nph.13230

Jacobi, C. M., do Carmo, F. F., Vincent, R. C., & Stehmann, J. R. (2007). Plant communities on ironstone outcrops: A diverse and endangered Brazilian ecosystem. *Biodiversity and Conservation*, *16*(7), 2185–2200. https://doi.org/10.1007/s10531-007-9156-8

Johnson, M. T. J., & Stinchcombe, J. R. (2007). An emerging synthesis between community ecology and evolutionary biology. *Trends in Ecology and Evolution*, *22*(5), 250–257. https://doi.org/10.1016/j.tree.2007.01.014

Kessous, I. M., Neves, B., Couto, D. R., Paixão-Souza, B., Pederneiras, L. C., Moura, R. L., Barfuss, M. H. J., Salgueiro, F., & Costa, A. F. (2019). Historical biogeography of a Brazilian lineage of Tillandsioideae (subtribe Vrieseinae, Bromeliaceae): The Paranaean Sea hypothesized as the main vicariant event. *Botanical Journal of the Linnean Society*, *192*(4), 625–641. https://doi.org/10.1093/botlinnean/boz038

Larkin, M. A., Blackshields, G., Brown, N. P., Chenna, R., McGettigan, P. A., McWilliam, H., Valentin, F., Wallace, I. M., Wilm, A., Lopez, R., Thompson, J. D., Gibson, T. J., & Higgins, D. G. (2007). Clustal W and Clustal X version 2.0. *Bioinformatics*, *23*(21), 2947–2948. https://doi.org/10.1093/bioinformatics/btm404

Li, J., Huang, J. P., Sukumaran, J., & Knowles, L. L. (2018). Microevolutionary processes impact macroevolutionary patterns. *BMC Evolutionary Biology*, *18*(1), 1–8. https://doi.org/10.1186/s12862-018-1236-8.

Librado, P., & Rozas, J. (2009). DnaSP v5: A software for comprehensive analysis of DNA polymorphism data. *Bioinformatics*, *25*(11), 1451–1452. https://doi.org/10.1093/bioinformatics/btp187

Lisiecki, L. E., & Raymo, M. E. (2007). Plio-Pleistocene climate evolution: Trends and transitions in glacial cycle dynamics. *Quaternary Science Reviews*, *26*(1–2), 56–69. https://doi.org/10.1016/j.quascirev.2006.09.005

Liu, Y., Hu, J., Li, S. H., Duchen, P., Wegmann, D., & Schweizer, M. (2016). Sino-Himalayan mountains act as cradles of diversity and immigration centres in the diversification of parrotbills (Paradoxornithidae). *Journal of Biogeography*, *43*(8), 1488–1501. https://doi.org/10.1111/jbi.12738

Machado, T. M., Loiseau, O., Paris, M., Weigand, A., Versieux, L. M., Stehmann, J. R., Lexer, C., & Salamin, N. (2020). Systematics of *Vriesea* (Bromeliaceae): Phylogenetic relationships based on nuclear gene and partial plastome sequences. *Botanical Journal of the Linnean Society*, *192*(4), 656–674. https://doi.org/10.1093/botlinnean/boz102

Madriñán, S., Cortés, A. J., & Richardson, J. E. (2013). Páramo is the world's fastest evolving and coolest biodiversity hotspot. *Frontiers in Genetics*, *4*, 1–7. https://doi.org/10.3389/fgene.2013.00192

Magalhães Junior, A. P., de Paula Barros, L. F., & Felippe, M. F. (2015). Southern Serra do Espinhaço: The impressive plateau of quartzite ridges. In B. Vieira, A. Salgado, & L. Santos (Eds.), *Landscapes and Landforms of Brazil* (pp. 359–370). Springer.

Miller, M. A., Pfeiffer, W., & Schwartz, T. (2010). Creating the CIPRES Science Gateway for inference of large phylogenetic trees. In *2010 Gateway Computing Environments Workshop, GCE 2010* (pp. 1–8). IEEE. https://doi.org/10.1109/GCE.2010.5676129

Mota, M. R., Pinheiro, F., Leal, B. S. S., Sardelli, C. H., Wendt, T., & Palma-Silva, C. (2020). From micro- to macroevolution: Insights from a Neotropical bromeliad with high population genetic structure adapted to rock outcrops. *Heredity*, *125*(5), 353–370. https://doi.org/10.1038/s41437-020-0342-8

Muellner-Riehl, A. N., Schnitzler, J., Kissling, W. D., Mosbrugger, V., Rijsdijk, K. F., Seijmonsbergen, A. C., Versteegh, H., & Favre, A. (2019). Origins of global mountain plant biodiversity: Testing the 'mountain-geobiodiversity hypothesis'. *Journal of Biogeography*, *46*(12), 2826–2838. https://doi.org/10.1111/jbi.13715

Nascimento, A. C., Chaves, A. V., Fortes Leite, F. S., Eterovick, P. C., & dos Santos, F. R. (2018). Past vicariance promoting deep genetic divergence in an endemic frog species of the espinhaço range in Brazil: The historical biogeography of *Bokermannohyla saxicola* (Hylidae). *PLoS One*, *13*(11), 1–19. https://doi.org/10.1371/journal.pone.0206732

Peakall, R., & Smouse, P. E. (2012). GenAlEx 6.5: Genetic analysis in Excel. Population genetic software for teaching and research–an update. *Bioinformatics*, *28*(19), 2537–2539.

Perrigo, A., Hoorn, C., & Antonelli, A. (2020). Why mountains matter for biodiversity. *Journal of Biogeography*, *47*(2), 315–325. https://doi.org/10.1111/jbi.13731

Philcox, D. (1992). Notes on South American Bromeliaceae. *Kew Bulletin*, *47*(2), 261. https://doi.org/10.2307/4110667

Pinheiro, F., Cozzolino, S., de Barros, F., Gouveia, T. M. Z. M., Suzuki, R. M., Fay, M. F., & Palma-Silva, C. (2013). Phylogeographic structure and outbreeding depression reveal early stages of reproductive isolation in the neotropical orchid *Epidendrum denticulatum*. *Evolution*, *67*(7), 2024–2039.

Pirani, J. R., Mello-Silva, R., & Giulietti, A. M. (2003). Flora de Grão-Mogol, Minas Gerais, Brasil. *Boletim De Botânica Da Universidade De São Paulo*, *21*(1), 1–24. https://doi.org/10.11606/issn.2316-9052.v21i1p1-24

Prell, W. L. (1984). Covariance patterns of foraminiferal dgr18O: An evaluation of Pliocene ice volume changes near 3.2 million years ago. *Science*, *226*(4675), 692–694.

Pritchard, J. K., Stephens, M., & Donnelly, P. (2000). Inference of population structure using multilocus genotype data. *Genetics*, *155*, 945–959. https://doi.org/10.1093/genetics/155.2.945

R Core Team. (2019). *R: A language and environment for statistical computing*. R Foundation for Statistical Computing.

Rahbek, C., Borregaard, M. K., Antonelli, A., Colwell, R. K., Holt, B. G., Nogues-Bravo, D., Rasmussen, C. M. Ø., & Fjeldså, J. (2019). Building mountain biodiversity: Geological and evolutionary processes. *Science*, *365*(6458), 1114–1119.

Rambaut, A., & Drummond, A. J. (2016). TreeAnnotator version 1.8. Available at: http://beast.community/programs

Rambaut, A., Drummond, A. J., Xie, D., Baele, G., & Suchard, M. A. (2018). Posterior summarization in Bayesian phylogenetics using tracer 1.7. *Systematic Biology*, *67*(5), 901–904. https://doi.org/10.1093/sysbio/syy032

Raymond, M., & Rousset, F. (1995). GENEPOP (Version 1.2): Population genetics software for exact tests and ecumenicism. *Journal of Heredity*, *86*(3), 248–249.

Ribeiro, P. L., Rapini, A., Damascena, L. S., & van Den Berg, C. (2014). Plant diversification in the Espinhaço Range: Insights from the biogeography of *Minaria* (Apocynaceae). *Taxon*, *63*(6), 1253–1264.

Rull, V. (2005). Biotic diversification in the Guayana Highlands: A proposal. *Journal of Biogeography*, *32*(6), 921–927. https://doi.org/10.1111/j.1365-2699.2005.01252.x

Rull, V. (2011). Neotropical biodiversity: Timing and potential drivers. *Trends in Ecology and Evolution*, *26*(10), 508–513. https://doi.org/10.1016/j.tree.2011.05.011

Rull, V., & Vegas-Vilarrúbia, T. (2020). The Pantepui "Lost World": Towards a biogeographical, ecological and evolutionary synthesis of a pristine Neotropical sky-island archipelago. In V. Rull, & A. C. Carnaval (Eds.), *Neotropical Diversification: Patterns and Processes* (pp. 369–413). Springer, Charm.

Saadi, A. (1995). A geomorfologia da Serra do Espinhaço em Minas Gerais e de suas margens. *Geonomos*, *43*(1), 41–63. https://doi.org/10.18285/geonomos.v3i1.215

Salerno, P. E., Ron, S. R., Señaris, J. C., Rojas-Runjaic, F. J. M., Noonan, B. P., & Cannatella, D. C. (2012). Ancient tepui summits harbor young rather than old lineages of endemic frogs. *Evolution*, *66*(10), 3000–3013. https://doi.org/10.1111/j.1558-5646.2012.01666.x

Schoville, S. D., Roderick, G. K., & Kavanaugh, D. H. (2012). Testing the "Pleistocene species pump" in alpine habitats: Lineage diversification of flightless ground beetles (Coleoptera: Carabidae: *Nebria*) in relation to altitudinal zonation. *Biological Journal of the Linnean Society*, *107*(1), 95–111. https://doi.org/10.1111/j.1095-8312.2012.01911.x

Sedano, R. E., & Burns, K. J. (2010). Are the Northern Andes a species pump for Neotropical birds? Phylogenetics and biogeography of a clade of Neotropical tanagers (Aves: Thraupini). *Journal of Biogeography*, *37*(2), 325–343. https://doi.org/10.1111/j.1365-2699.2009.02200.x

Sexton, J. P., Hangartner, S. B., & Hoffmann, A. A. (2014). Genetic isolation by environment or distance: Which pattern of gene flow is most common? *Evolution*, *68*(1), 1–15. https://doi.org/10.1111/evo.12258

Silva, G. A. R. S., Antonelli, A., Lendel, A., Moraes, E. M., & Manfrin, M. H. (2018). The impact of early Quaternary climate change on the diversification and population dynamics of a South American cactus species. *Journal of Biogeography*, *45*(1), 75–88. https://doi.org/10.1111/jbi.13107

Silva, K. R., Versieux, L. M., & Oriani, A. (2020). Morphological and anatomical variations of roots, leaves, peduncles, and peduncle bracts in the *Vriesea oligantha* complex (Bromeliaceae): Perspectives for taxonomy. *Systematic Botany*, *45*(4), 779–793.

Silveira, F. A. O., Dayrell, R. L. C., Fiorini, C. F., Negreiros, D., & Borba, E. L. (2020). Diversification in ancient and nutrient-poor Neotropical ecosystems: How geological and climatic buffering shaped plant diversity in some of the world's neglected hotspots. In V. Rull, & A. C. Carnaval (Eds.), *Neotropical Diversification: Patterns and Processes* (pp. 329–368). Springer, Charm.

Tel-Zur, N., Abbo, S., Myslabodski, D., & Mizrahi, Y. (1999). Modified CTAB procedure for DNA isolation from epiphytic cacti of genera *Hylocereus* and *Selenicereus* (Cactaceae). *Plant Molecular Biology, 17*, 249–254.

Testo, W. L., Sessa, E., & Barrington, D. S. (2019). The rise of the Andes promoted rapid diversification in Neotropical *Phlegmariurus* (Lycopodiaceae). *New Phytologist, 222*(1), 604–613.

Vanzolini, P. E., & Williams, E. E. (1970). South American anoles: The geographic differentiation and evolution of the anolis *Chrysolepis* species group (Sauria, Iguanidae). *Arquivos De Zoologia, 19*(3–4), 125. https://doi.org/10.11606/issn.2176-7793.v19i1-2p1-176

Vasconcelos, T. N. C., Alcantara, S., Andrino, C. O., Forest, F., Reginato, M., Simon, M. F., & Pirani, J. R. (2020). Fast diversification through a mosaic of evolutionary histories characterizes the endemic flora of ancient Neotropical mountains. *Proceedings of the Royal Society B: Biological Sciences, 287*(1923), 20192933. https://doi.org/10.1098/rspb.2019.2933

von Humboldt, A. (1807). *Ideen zu einer Geographie der Pflanzen nebst einem Naturgemälde der Tropenländer : auf Beobachtungen und Messungen gegründet, welche vom 10ten Grade nördlicher bis zum 10ten Grade südlicher Breite, in den Jahren 1799, 1800, 1801, 1802 und 1803 angestellt worden sind, von Al. von Humboldt und A. Bonpland. Bearbeitet und herausgegeben von dem erstern.* Cotta.

Wang, I. J., & Bradburd, G. S. (2014). Isolation by environment. *Molecular Ecology, 23*(23), 5649–5662. https://doi.org/10.1111/mec.12938

Weir, B. S., & Cockerham, C. C. (1984). Estimating F-statistics for the analysis of population structure. *Evolution, 38*(6), 1358.

Wilson, G. A., & Rannala, B. (2003). Bayesian inference of recent migration rates using multilocus genotypes. *Genetics, 163*(3), 1177–1191. https://doi.org/10.1093/genetics/163.3.1177

Wright, S. (1943). Isolation by distance. *Genetics, 28*(2), 114–138. https://doi.org/10.1093/genetics/28.2.114

Ye, X., Ma, P., Yang, G., Guo, C., Zhang, Y., Chen, Y., Guo, Z., & Li, D. (2019). Rapid diversification of alpine bamboos associated with the uplift of the Hengduan Mountains. *Journal of Biogeography, 46*(12), 2678–2689. https://doi.org/10.1111/jbi.13723

Zappi, D. C., Lucas, E., Stannard, B. L., Lughadha, E. N., Pirani, J. R., Queiroz, L. P., Atkins, S., Hind, D., Giulietti, A. M., Harley, R. M., & De Carvalho, A. M. (2003). Lista das plantas vasculares de Catolés, Chapada Diamantina, Bahia, Brasil. *Boletim De Botânica Da Universidade De São Paulo, 21*(2), 345–398. https://doi.org/10.11606/issn.2316-9052.v21i2p345-398

Zappi, D. C., Moro, M. F., Meagher, T. R., & Nic Lughadha, E. (2017). Plant biodiversity drivers in Brazilian campos rupestres: Insights from phylogenetic structure. *Frontiers in Plant Science, 8*, 1–15. https://doi.org/10.3389/fpls.2017.02141

BIOSKETCH

Marcos Vinicius Dantas-Queiroz is a PhD candidate at São Paulo State University, Brazil. His broader research interests include biogeography, phylogeography, ecology and evolution of Neotropical plants, with emphasis on understanding the processes responsible for origin and diversification of species. All authors share a common interest in understanding the processes and mechanisms responsible for the generation and maintenance of biodiversity using mainly bromeliads as Neotropical models to reach this goal.

Author contributions: M.V.D.Q., C.P.S. and L.M.V. conceived the ideas and designed the study; M.V.D.Q., T.C.S. and L.M.V. conducted fieldwork and collected the data. M.V.D.Q., T.C.S., B.S.S.L., C.J.N.C., T.N.C.V. and C.P.S. analyzed the data. M.V.D.Q. wrote the manuscript, and all authors helped improve the final version. The authors declare no conflict of interest.

SUPPORTING INFORMATION

Additional supporting information may be found online in the Supporting Information section.

How to cite this article: Dantas-Queiroz MV, Cacossi Td, Leal BS, et al. Underlying microevolutionary processes parallel macroevolutionary patterns in ancient neotropical mountains. *J Biogeogr.* 2021;00:1–16. https://doi.org/10.1111/jbi.14154